Proceedings IRF2018: 6th International Conference Integrity-Reliability-Failure
Lisbon/Portugal 22-26 July 2018. Editors J.F. Silva Gomes and S.A. Meguid
Publ. INEGI/FEUP (2018); ISBN: 978-989-20-8313-1

PAPER REF: 7192

APPLICATION OF A COMPLETE STRUCTURAL HEALTH MONITORING CHAIN ON THE CANADIAN RIVIÈRE-AUX-MULETS BRIDGE NUMERICAL MODEL SUBJECTED TO A SEISMIC LOAD

Farouk Frigui[1,2(*)], Jean-Pierre Faye[1], Carmen Martin[1], Olivier Dalverny[1], François Peres[1], Sébastien Judenherc[2]

[1]Ecole Nationale d'Ingénieurs de Tarbes, LGP, 47 avenue d'Azereix, 65016 Tarbes, France
[2]STANEO, 2 rue Marcel Langer 31600 Seysses, France
[(*)]*Email:* ffrigui@enit.fr

ABSTRACT

The surveillance of civil engineering structures has become increasingly important over the last decade. Nowadays, several methods and means of Structural Health Monitoring (SHM) exist. They help to detect, localize and quantify damage, and predict the remaining service life of structures. One of the major challenges in the SHM field of civil engineering structures is to define a global and reliable methodology of damage detection and localization. In this paper, a complete chain of surveillance is set up on a three-dimensional Finite Element (FE) model of the Canadian Rivière-Aux-Mulets bridge, created with the ABAQUS software. The structure is damaged by a true seismic signal and a set of Vibration-Based Damage Detection Methods (VBDDM) is applied to detect and to localize the damage.

Keywords: Structural Health Monitoring (SHM), Operational Modal Analysis (OMA), dynamic behavior, seismic load.

INTRODUCTION

Structural damage in civil engineering is essentially related to the environment where the structure is located. In fact, temperature change, aging of materials, human activities and natural disasters have a direct influence on the performance of structures. Therefore, civil engineering supervision has become very important over the last decade. Today, there are several methods of monitoring allowing the understanding of the structure's dynamic behaviour. These methods, also called Vibration-Based Damage Detection Methods (VBDDM), consist in the monitoring of the temporal evolution of dynamic characteristics such as eigen-frequencies and mode shapes (Ndambi, 2002). These dynamic characteristics can be identified on a real structure from its output response using Operational Modal Analysis (OMA) techniques, under white noise assumption.

In this context, we present the monitoring of the numerical model of the Canadian Rivière-aux-Mulets bridge subjected to a seismic load. The experimental SHM chain was carried out numerically. OMA algorithms were implemented in MATLAB to identify eigen-frequencies and mode shapes from these responses: the Stochastic Subspace Identification (SSI-COV) method was used to identify eigen-frequencies and the Frequency Domain Decomposition (FDD) was used to identify mode shapes. Identification results were compared to that of Abaqus. Finally, the detection and the localization of damages were made by applying the VBDDM methods, namely: eigen-frequencies method (Δf), Modal Assurance Criterion

(MAC), Mode Shape Curvatures Method (MSCM), Curvature Damage Factor (CDF) and the Flexibility Curvature method (FC).

1. DAMAGE DETECTION AND LOCALIZATION:

The surveillance methods, most commonly used in civil engineering, are based on the relation that exists between the change of the physical properties, and the variations of dynamic characteristics: variations of eigen-frequencies, mode shapes and damping. Thanks to this causal link, monitoring the evolution of these characteristics represents an accurate method of health monitoring (Carden, 2004). These techniques help choosing actions of rehabilitation on damaged structures, leading consequently to an optimization of maintenance costs. This principle has received considerable attention during the past two decades. However, the problem lies in the setup of a correct correlation between the variations of the dynamic characteristics, the appearance of the damage and its location.
Here in, we present a non-exhaustive list of detection and localization methods commonly used in civil engineering. The implementation, advantages and disadvantages of each method are presented.

1.1. Eigen-frequencies changes (Δf)

The damage induces a change in the structure's behaviour, particularly a shift of the eigen-frequencies. This dynamic characteristic reflects the overall behaviour of the structure. Thus, the monitoring of the frequencies is a sensitive damage indicator. Eigen-frequencies method is computed as follows (Salawu, 1997):

$$\Delta \mathrm{f} = \frac{\mathrm{f_i^u} - \mathrm{f_i^d}}{\mathrm{f_i^u}} \tag{1}$$

Where f_i^u and f_i^d are respectively the eigen-frequencies of the ith mode. *u* and *d* denote respectively the undamaged and the damaged state.

Since the eigen-frequency is an intrinsic property of the structure and no spatial information are required for its application, this technique addresses the overall structure and, as a result, allows only detection of damage (Farrar, 2001).

1.2. Modal Assurance Criterion (MAC)

Since the mode shapes are sensitive to the structure's state, their follow-up allows detecting damages. In order to compare the mode shapes of a healthy structure to those of the damaged one, the MAC can be used. It's computed as follows (Allemang, 1982):

$$\mathrm{MAC_{jk}} = \frac{[\sum_{\mathrm{i=1}}^{\mathrm{n}} [\Psi_\mathrm{u}]_\mathrm{i}^\mathrm{j} [\Psi_\mathrm{d}]_\mathrm{i}^\mathrm{K}]^2}{\sum_{\mathrm{i=1}}^{\mathrm{n}} ([\Psi_\mathrm{u}]_\mathrm{i}^\mathrm{j})^2 \sum_{\mathrm{i=1}}^{\mathrm{n}} ([\Psi_\mathrm{d}]_\mathrm{i}^\mathrm{k})^2} \tag{2}$$

With Ψ_u and Ψ_d are respectively the undamaged and the damaged sets of mode shapes. *n* is the number of modes.

MAC is used to determine the similarity of two mode shapes. If the mode shapes are identical, then MAC will have a value of 1. If the mode shapes are different due to the damage, the

MAC value will be less than 1 (Pastor, 2012). The most interesting values are those of the diagonal because they reflect the correlation between the shapes of the same mode. This method has two major disadvantages. In the first place, for low damage and according to its position, it can be detected by the MAC method using higher order modes (Lam, 1998). These modes are more sensitive to damage and difficult to identify experimentally. In the second place, it only allows detection of damages without localization.

1.3. Mode Shape Curvature Method (MSCM)

This method is very sensitive to small disturbances caused by damages (Salane, 1990). It can be computed using the central difference approximation as follows (Pandey, 1991):

$$\Psi''_{i,j} = \frac{(\Psi_{i+1,j} - 2\Psi_{i,j} + \Psi_{i-1,j})}{h^2} \tag{3}$$

$$\Delta\Psi''_{i,j} = |\Psi''^{u}_{i,j} - \Psi''^{d}_{i,j}| \tag{4}$$

Where $\Psi_{i,j}$ and $\Psi''_{i,j}$ are respectively the displacement and the mode shape curvature at the i^{th} node and j^{th} mode. h is the distance between two consecutive measurement nodes. u and d denote respectively the undamaged and damaged structure.

Unlike the methods presented above, this technique allows to locate the damage. However, the choice of the mode is very important. Indeed, some modes are less sensitive to damage than others and can induce misleading information (Foti, 2013)

1.4. Curvature Damage Factor (CDF)

In order to avoid the problem of choosing an appropriate mode in MSCM and to reach global information concerning the damage, one can use the Curvature Damage Factor (CDF) (Wahab, 1999). It consists in averaging the variations of the mode shape curvature with respect to the number of considered modes N:

$$\mathrm{CDF} = \frac{\sum_{n=1}^{N} |\Psi''^{u}_{i,j} - \Psi''^{d}_{i,j}|}{N} \tag{5}$$

1.5. Flexibility Curvature (FC)

Damage in the structure induces and increases in its flexibility. Thus, follow-up flexibility curvature can allow damage detection and localization. Flexibility matrix can be computed as follows (Pandey, 1995):

$$F = \sum_{i=1}^{n} \frac{1}{w_i^2} \Psi_i \Psi_i^t \tag{6}$$

Where w_i is the i^{th} eigen-frequency and Ψ is the mode shape matrix mass-normalized to unity ($\Psi^t M \Psi = 1$).

The flexibility converges rapidly by increasing the frequency, thus a few lower modes provide a good estimation of the flexibility matrix. Generally, the first two modes are sufficient.

The flexibility curvature method is computed following the steps below:

1- Computing the flexibility variation matrix: $\Delta F = F_u - F_d$ (7)

2- Computing the maximum absolute value: $\overline{\Upsilon_j} = max_i\,|\Delta F_{ij}|$ (Ndambi, 2002) (8)

3- Computing the flexibility curvature: $\overline{\gamma_j''} = \frac{\overline{\gamma_{j-1}} + \overline{\gamma}_{j+1} - 2\overline{\gamma}_j}{h^2}$ (Zhang, 1995) (9)

With F_u is the initial flexibility matrix corresponding to the undamaged structure and F_d is the final flexibility matrix corresponding to the damaged structure. *h* is the distance between two consecutive measurement nodes.

2. OPERATIONAL MODAL ANALYSIS (OMA) TECHNIQUES: The SHM techniques, previously presented, use natural frequencies and mode shapes. These characteristics can be identified experimentally using Operational Modal Analysis (OMA) methods (Cunha, 2005). In this section, we present two methods essentially: the Stochastic Subspace Identification technique (SSI) for the identification of eigen-frequencies and the Frequency Domain Decomposition (FDD) for the identification of mode shapes. Both techniques were chosen for their efficiency and robustness (Greiner, 2009; Ghalishooyan, 2015).

2.1. The Stochastic Subspace Identification (SSI):

In the case of a time-invariant linear dynamic model, the state-space model in discretized domain can be written as (Basseville, 2001):

$$\begin{cases} x_{(k+1)} = Ax_{(k)} + w_{(k)} \\ y_{(k)} = Cx_{(k)} + q_{(k)} \end{cases} \quad (10)$$

Where $x_{(k+1)}$ is the *(2n×1)* state vector at the time instant *(k+1)ΔT*, *ΔT* is the sampling period, $y_{(k)}$ is the *(l ×1)* output vector at the time instant *kΔT*. *A* is the transition matrix, *C* is the observation matrix. $w \in R^{2n\times 1}$and $q \in R^{l\times 1}$ are respectively the process and the measurement noises and are assumed to be white noises.

The transition matrix *A* contains all the modal information. Indeed, its eigenvalues λ_i are related to the eigen-frequencies through the next equation (Peeters, 1995; Peeters, 2000):

$$f_i = \sqrt{Re\left(\frac{ln(\lambda_i)}{\Delta T}\right)^2 + Im\left(\frac{ln(\lambda_i)}{\Delta T}\right)^2} \Big/ 2\pi \quad (11)$$

Where *Re* and *Im* denote respectively the real part and the imaginary part.

The purpose of the SSI algorithm is to identify the transition matrix *A* from the structure's response. This can be achieved using the covariance matrix of the outputs $y_{(k+i)}$ and $y_{(k)}$. It can be written as (Xie, 2016):

$$\Lambda_i = CA^{i-1}G \quad (12)$$

Where $G = A\Sigma_{xx}C^t + S$, Σ_{xx} is the covariance matrix of the state vector $x_{(k)}$ and S is the covariance matrix of $w_{(k)}$ and $q_{(k)}$. t denotes the transpose operator.

The SSI's algorithm is setup following these steps (Kuts, 2016):

- Step 1: Gathering the covariance matrices of the outputs into the Hankel block matrix *H* as follows:

$$\mathrm{H} = \begin{bmatrix} \mathrm{CA^0G} & \mathrm{CA^1G} & \dots & \mathrm{CA^{q-1}G} \\ \mathrm{CA^1G} & \vdots & \vdots & \mathrm{CA^qG} \\ \vdots & \vdots & \vdots & \vdots \\ \mathrm{CA^pG} & \mathrm{CA^{p+1}G} & \dots & \mathrm{CA^{p+q-1}G} \end{bmatrix} \tag{13}$$

- Step 2: Decomposition of the Hankel block matrix *H* into three matrices *U*, *S* and *V* using the Single Value Decomposition (SVD):

$$\mathrm{H} = \mathrm{USV^t} = \mathrm{U_1 {S_1}^{0.5} {S_1}^{0.5} {V_1}^t} = \mathrm{O} * \mathrm{K} \tag{14}$$

Where *O* is the observability matrix and *K* is the controllability matrix.

- Step 3: Identification of the observability matrix *O* using equation (14)

$$\mathrm{O} = \mathrm{U_1 {S_1}^{0.5}} \tag{15}$$

- Step 4: Computing the shifted matrices $O^{\uparrow}$ and $O^{\downarrow}$. $O^{\uparrow}$ is obtained by removing the last block row and $O^{\downarrow}$ is obtained by removing the first block row of the observability matrix *O* as follows:

$$\mathrm{O^{\uparrow}} = \begin{pmatrix} \mathrm{C} \\ \mathrm{CA} \\ \mathrm{CA^2} \\ \vdots \\ \mathrm{CA^{p-1}} \end{pmatrix}, \mathrm{O^{\downarrow}} = \begin{pmatrix} \mathrm{CA} \\ \mathrm{CA^2} \\ \vdots \\ \vdots \\ \mathrm{CA^p} \end{pmatrix} \tag{16}$$

- Step 5: Identification of the transition matrix *A*

$$\mathrm{A} = \mathrm{O^{\uparrow} {O^{\downarrow}}^{\#}} \tag{17}$$

Where # denotes the Moore-Penrose pseudo-inverse.

- Step 6: Identification of eigen-frequencies using equation (11).

2.2. The Frequency Domain Decomposition (FDD):

Under assumption of a white noise excitation, mode shapes can be estimated from the spectral density (Brincker, 2000). The inputs $x(t)$ and the outputs $y(t)$ are related through the next equation:

$$\mathrm{G_{yy}(jw)} = [\mathrm{FRF(jw)}][\mathrm{G_{xx}(jw)}][\mathrm{FRF(jw)}]^{\mathrm{t}} \tag{18}$$

Where $G_{xx}(jw)$ and $G_{yy}(jw)$ are the input and the output Power Spectral Density (PSD) matrices. $G_{xx}(jw)$ is constant given that excitation is considered as a zero-mean white noise. $FRF(jw)$ is the Frequency Response Function matrix.

Under the assumption of a lightly damped structure and white noise excitation, $G_{yy}(jw)$ can be written as follows:

$$\mathrm{G_{yy}(jw)} = \sum_{\mathrm{k} \in (\mathrm{sub(w)})} \frac{\mathrm{d_k}\phi_\mathrm{k}\phi_\mathrm{k}^{\mathrm{t}}}{\mathrm{jw} - \lambda_\mathrm{k}} + \frac{\mathrm{d_k^*}\phi_\mathrm{k}^*\phi_\mathrm{k}^{*\mathrm{t}}}{\mathrm{jw} - \lambda_\mathrm{k}^*} \tag{19}$$

Where d_k is a scalar constant and $sub(w)$ is a set of modes that contribute at a particular frequency. ϕ_k is the mode shapes matrix, $\lambda_k = -\sigma_k + jw_{dk}$ are poles and w_{dk} is the damped natural frequency. The superscripts * and *t* denote respectively the complex conjugate and the transpose operator.

The FDD algorithm is executed following these steps:

- Step 1: Computing the Power Spectral Density matrix $Gyy(jw)$:

$$\mathrm{Gyy(jw)} = \begin{bmatrix} \mathrm{PSD_{11}(jw)} & \mathrm{CSD_{12}(jw)} & \mathrm{CSD_{13}(jw)} & \mathrm{CSD_{14}(jw)} \\ \mathrm{CSD_{21}(jw)} & \mathrm{PSD_{22}(jw)} & \mathrm{CSD_{23}(jw)} & \mathrm{CSD_{24}(jw)} \\ \mathrm{CSD_{31}(jw)} & \mathrm{CSD_{32}(jw)} & \mathrm{PSD_{33}(jw)} & \mathrm{CSD_{34}(jw)} \\ \mathrm{CSD_{41}(jw)} & \mathrm{CSD_{42}(jw)} & \mathrm{CSD_{43}(jw)} & \mathrm{PSD_{44}(jw)} \end{bmatrix} \tag{20}$$

  Where $PSD(jw)$ denotes the power spectral density and $CSD(jw)$ denotes the Cross Spectral Density. $Gyy(jw)$ is the Power spectral density matrix of 4 measured degree of freedom.
- Step 2: Performing SVD decomposition of $Gyy(jw)$ at eigen-frequencies (Wang, 2016):

$$\mathrm{G_{yy}(jw)} = [\phi][\Sigma][\phi]^{\mathrm{H}} \tag{21}$$

  Where the diagonal value of $[\Sigma]$ are the singular values and the columns of ϕ are the singular vectors.
- Step 3: If only one mode is dominating at a particular frequency, then only one singular value will be dominating. Thus the mode shape Ψi corresponds to the first eigenvector (Gade, 2005):

$$\Psi_i = \phi_{i1} \tag{22}$$

3. NUMERICAL SIMULATION:

The Rivière-aux-Mulets bridge, located on Highway 15 in Sainte-Adèle in the north-west of Montreal - CANADA, was modelled on Abaqus software and the damage was introduced by a true seismic load (Figure 1). The model consists of three concrete piers and three concrete spans. The left and right spans are *40.8 m* long and the central span is *80.4 m* long (Talbot, 2005). The north and south abutments have not been modelled. The span-abutments and span-pier connections are modelled by spring elements.

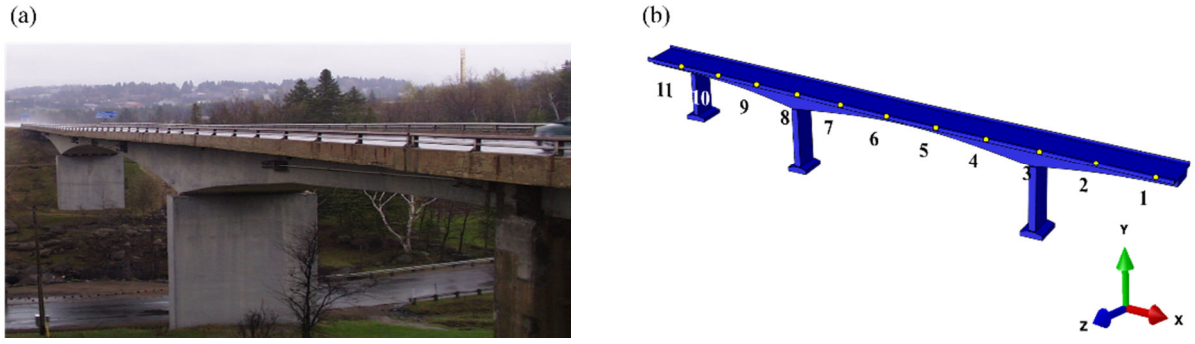

Fig. 1 - Rivière-Aux-Mulets bridge: (a) Street view; (b) Numerical model and location of the 11 sensors.

The L'Aquila earthquake accelerogram is used in this numerical simulation. The earthquake occurred in the Abruzzo region in Italy. Its magnitude rose to 6.3 on the moment magnitude scale. The earthquake damaged about 10,000 buildings making this earthquake the deadliest in Italy. The signal recorded at the AQV station was used to damage the numerical model (Figure 2). The purpose being to damage the structure, the signal amplitude is reduced to 50% and only 10 seconds of the signal are used to excite the model in the $\vec{x}$ and $\vec{z}$ directions. Eleven sensors were considered to record the response of the structure to white noise excitation before and after the damaging event in the $\vec{y}$ direction (Figure 1). They were placed in a linear and equidistant manner to have an accurate reflection of the mode shapes.

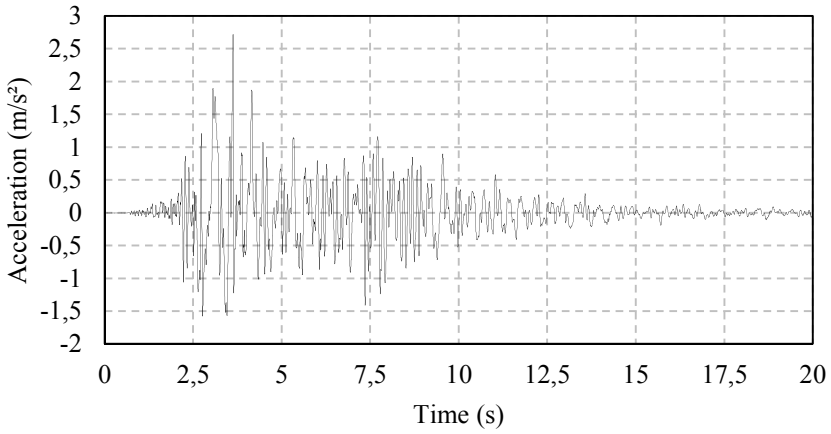

Fig. 2 - Vertical acceleration recorded at station AQV for 2009 L'Aquila earthquake, 2.5 mile from the earthquake epicenter (www.strongmotioncenter.org)

The numerical model takes into account the complex and non-linear behaviour of the concrete. The recognition of crack patterns is made through the elasto-plastic damage model: Concrete Damage Plasticity (CDP). The CDP is recommended for analysis of concrete structures subjected to cyclic loadings and is governed by the following equation (Jankowiak, 2005):

$$\sigma = (1 - \mathrm{d})\mathrm{D}_0^{\mathrm{el}} : (\varepsilon - \varepsilon^{\mathrm{pl}}) \qquad (23)$$

Where σ is Cauchy stresse tensor, d the scalar stiffness degradation variable, D_0^{el} the undamaged elastic stiffness of the material, ε the strain tensor and ε^{pl} the plastic strain tensor.

The major mechanisms of rupture for this model are tensile cracking and compression crushing. The damaged concrete response is characterized by two independent damage variables DamageT and DamageC, which are assumed to be dependent on plastic strain and

temperature. They range from 0 for undamaged material to 1 for completely damaged material. In the case of our work, no dependence on temperature is considered. The constitutive parameters of the concrete class B50 damaged plasticity model were used (Table 1).

Table 1 - Constitutive parameters of the concrete class B50 damaged plasticity model (Jankowiak, 2005)

Concrete compression hardening		**Concrete compression damage**		**Concrete tension stiffening**		**Concrete tension Damage**	
Stress [MPa]	**Crushing strain**	**DamageC**	**Crushing strain**	**Stress [MPa]**	**Cracking strain**	**DamageT**	**Cracking strain**
1.500E+01	0.000	0.000	0.000	1.999	0.000	0.000	0.000
2.020E+01	7.473E-05	0.000	7.473E-05	2.842	3.333E-05	0.000	3.333E-05
3.000E+01	9.885E-05	0.000	9.885E-05	1.870	1.604E-04	4.064E-01	1.604E-04
4.030E+01	1.541E-04	0.000	1.541E-04	8.627E-01	2.798E-04	6.964E-01	2.798E-04
5.001E+01	7.615E-04	0.000	7.615E-04	2.263E-01	6.846E-04	9.204E-01	6.846E-04
4.024E+01	2.558E-03	1.954E-01	2.558E-03	5.658E-02	1.087E-03	9.801E-01	1.087E-03
2.024E+01	5.675E-03	5.964E-01	5.675E-03				
5.258	1.173E-02	8.949E-01	1.173E-02				

After the seismic event, the model is found to be substantially damaged at the measuring nodes 3, 6 and 8 (Figure 3).

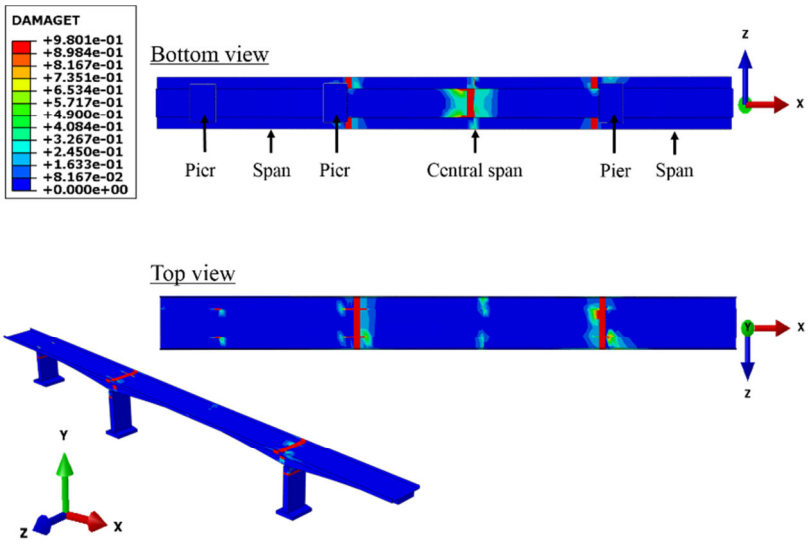

Fig. 3 - Distribution of tensile damage variable (DAMAGET)

The complete experimental SHM chain was carried out numerically. Meaning, the sensors were modelled by model-related nodes, and the response of the structure was recorded. In the first place, the structure was excited by a white noise in its undamaged state and its acceleration was recorded. In the second place, the structure was damaged by a seismic signal, excited by a white noise and its acceleration was recorded. Three types of analysis were used on Abaqus: Dynamic explicit to introduce the seismic excitation, Modal dynamics to record the structure's response and Frequency for modal analysis and to allow damage to appear. The different steps, mentioned above, are summarized in Figure 4.

We are interested only in the first two modes of bending in this direction afterwards. The complete SHM chain was performed using the accelerations of the structure in both states: the initial and the final state.

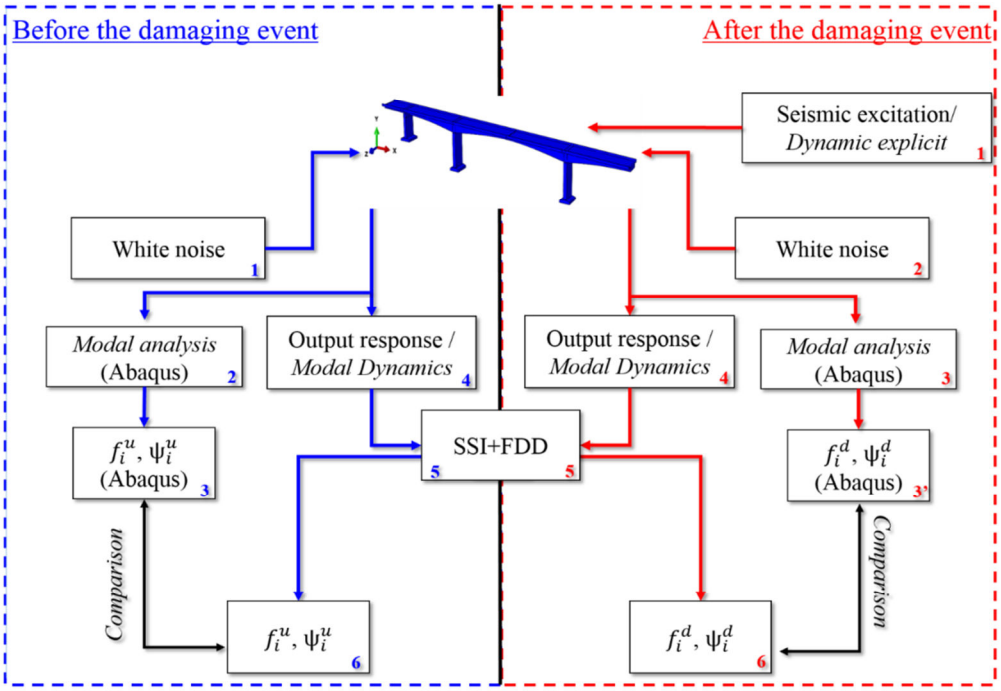

Fig. 4 - Flowchart explaining the different steps of the numerical studies allowing this work

4. RESULTS

4.1. Frequencies and mode shapes identification

The SSI algorithm was implemented using the response of the structure to a white noise.

The eigen-frequencies of the first modes have been successfully identified.

Table 2 - Result of eigen-frequencies identification using SSI algorithm

	Before the damage			**After the damaging event**		
Mode	Abaqus	SSI-COV	Error (%)	Abaqus	SSI-COV	Error (%)
1	1.52	1.52	0	1.49	1.48	0.5
2	2.57	2.59	-0.62	2.56	2.54	0.7

Results obtained by the finite element analysis and the Stochastic Subspace Identification method are very close (Table 2). The identification errors, not exceeding 1%, testify to the robustness of this AMO technique. These eigen-frequencies correspond to the 1st and 2nd bending modes in the $\vec{y}$ direction (Figure 5).

The FDD algorithm was implemented using SSI results and the same response of the structure to a white noise. Comparison of the first two estimated mode shapes with corresponding FE model ones is shown in Figure 6. Good agreement between the estimated mode shapes by FDD and the numerical ones can be observed.

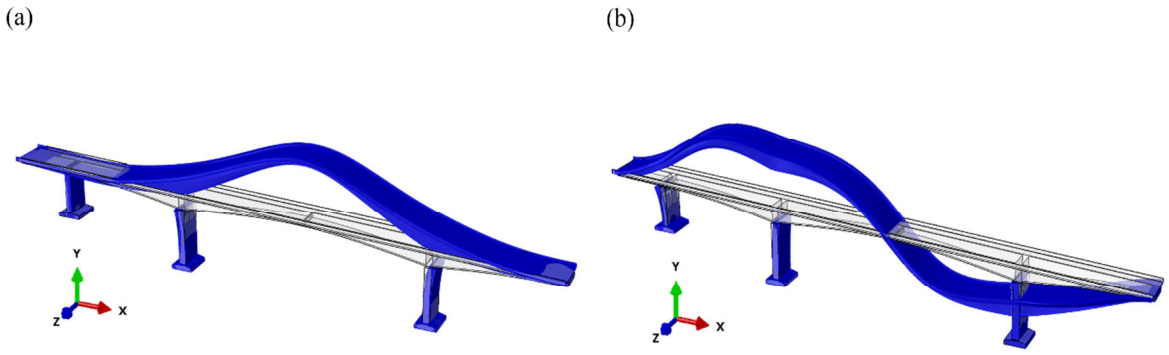

Fig. 5 - The mode shapes of vibration: (a) first bending mode 1.523 [Hz], (b) second bending mode 2.574 [Hz]

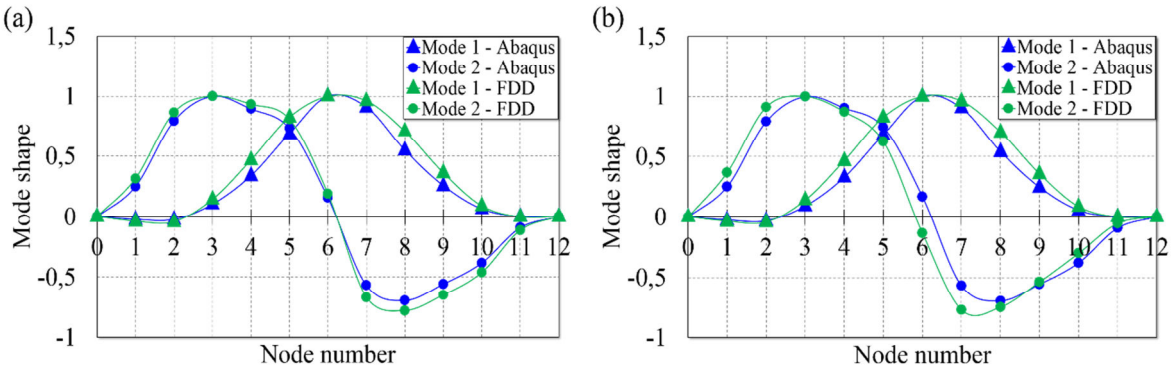

Fig. 6 - Table 1 Result of mode shape identification using FDD algorithm

4.2. Damage detection

Using the eigen-frequency method, the damage was detected thanks to a reduction of 2.63% in the first bending mode and a reduction of 1.93% in the second one (Figure 7). Unfortunately, in real life situations, such values do not allow to define the state of the structure. Damage is detected with confidence only when the shift of frequencies is 5% or more. Shifts lower than 5% can be explained by hygrothermal effects (Alvandi, 2003).

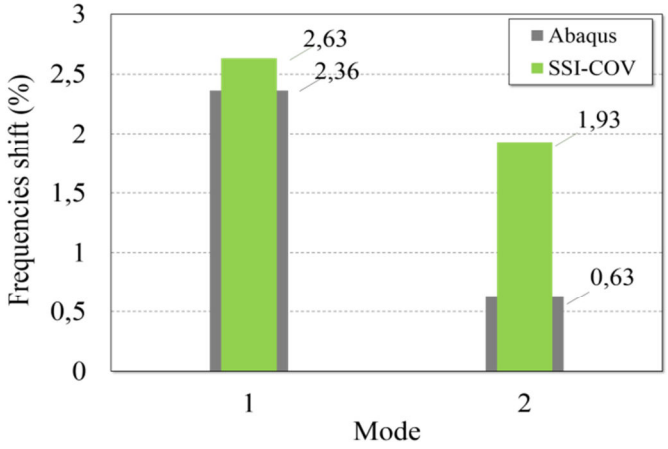

Fig. 7 - Shifts of the eigen-frequencies after the seismic event

The damages are not detected using the MAC criterion applied to the first mode shapes, since the values of MAC remain relatively close to 1 without any relevant indication of a defect (Figure 8a). Using Abaqus's results, the damages are detected in the 11th mode, indicated by a value 0.7 diagonally, which satisfies the detection condition (Figure 8b).

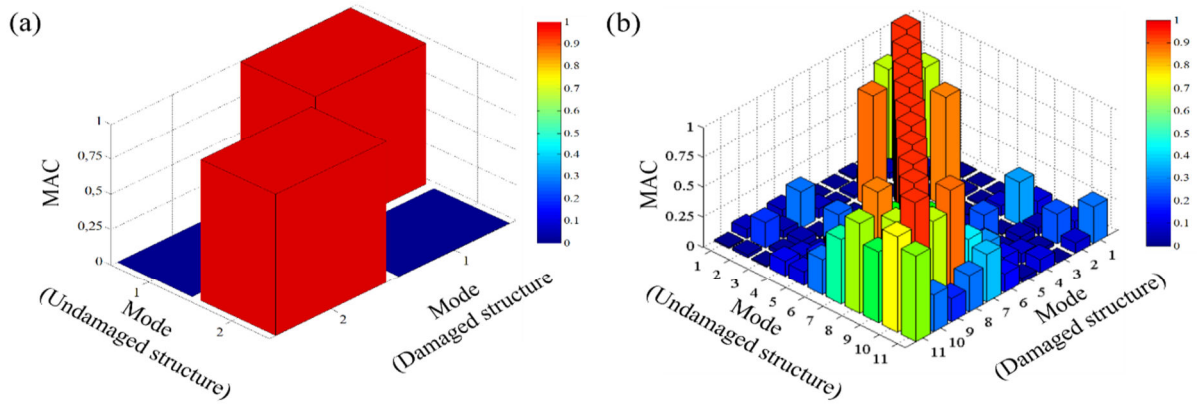

Fig. 8 - Modal Assurance Criterion: (a) two modes; (b) eleven modes

4.3. Damage localization

For the localization level, significant variations in the mode shape curvatures have been noted. These variations were located between node 6 and 8 in the first mode (Figure 9a) and around the node 4, 6 and 8 in the second mode (Figure 9b). Variations were also observed using the CDF between node 6 and 8 (Figure 10).

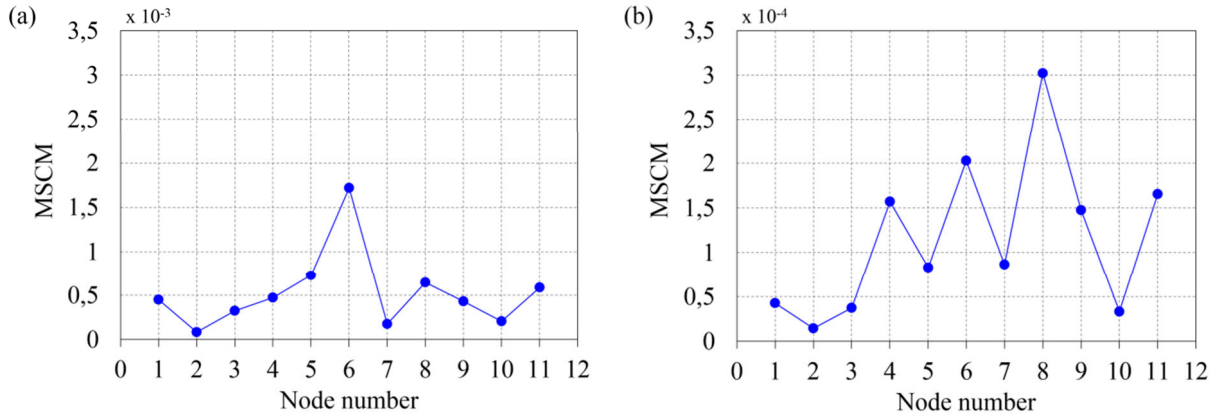

Fig. 9 - Mode Shape Curvature Method: (a) 1st bending mode, (b) 2nd bending mode

Using the first two modes, the flexibility matrices were calculated. Figure 11 shows the evolution of flexibility curvature along the bridge. Maximums are noted in the damaged areas (node 3, 6 and 8).

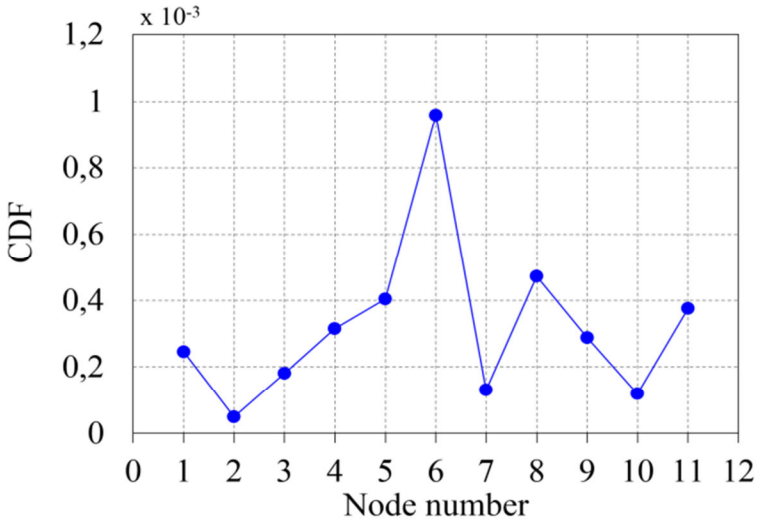

Fig. 10 - Curvature Damage Factor

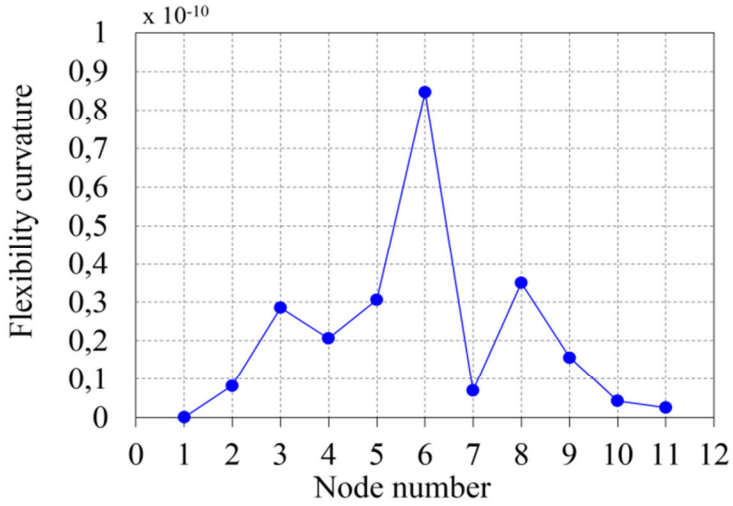

Fig. 11 - Flexibility curvature index

CONCLUSION

In this article, a complete chain of SHM of civil engineering structures was set up on a numerical model. The chosen model is the Rivière-Aux-Mulets bridge. It was damaged by the seismic signal of L'Aquila earthquake. The response of the healthy and the damaged structure, to a white noise excitation, was recorded. From its output only response, eigen-frequencies and modal deformations were identified by using Operational Modal Analysis techniques. These dynamic characteristics were used to define the state of the bridge. The study carried out allows us to highlight the following conclusions:

- As it has been reported in the literature, the Stochastic Subspace Identification technique and the Frequency Domain Decomposition technique proved to be very robust.

- The eigen-frequencies method has been able to detect the damage, but the reduction of the frequencies is weak. Experimentally, these variations can be caused by hygrothermal effects, without the structure being damaged.
- The damages were detected using the MAC method in the 11^{th} mode. This higher order mode is difficult to identify experimentally.
- In this test case, the flexibility curvature method showed the most accurate damage localization results.

ACKNOWLEDGMENTS

The study received financial support from the National Association of Research and Technology (ANRT). The authors are very thankful for this support.

REFERENCES

[1] Ndambi JM, Vantomme J, Harri, K. Damage assessment in reinforced concrete beams using eigenfrequencies and mode shape derivatives. Engineering Structures, 2002, 24(4), pp. 501-515.

[2] Carden EP, Fanning P. Vibration based condition monitoring: a review. Structural Health Monitoring, 2004, 3(4), pp. 355-377.

[3] Salawu OS. Detection of structural damage through changes in frequency: a review. Engineering Structures, 1997, 19(9), pp. 718-723.

[4] Farrar CR, Doebling SW, Nix DA. Vibration-based structural damage identification. Philosophical Transactions of the Royal Society of London A: Mathematical, Physical and Engineering Sciences, 2001, 359(1778), pp. 131-149.

[5] Alvandi A. Contribution à l'utilisation pratique de l'évaluation dynamique pour la détection d'endommagements dans les ponts, PhD thesis, Ecole des Ponts ParisTech, 2003.

[6] Allemang RJ, Brown DL. A correlation coefficient for modal vector analysis. In Proceedings of the 1st international modal analysis conference, 1, 1982, pp. 110-116.

[7] Pastor M, Binda M, Harčarik T. Modal assurance criterion. Procedia Engineering, 2012, 48, pp. 543-548.

[8] Lam HF, Ko JM, Wong CW. Localization of damaged structural connections based on experimental modal and sensitivity analysis. Journal of Sound and Vibration, 1998 210(1), pp. 91-115.

[9] Salane HJ, Baldwin Jr JW. Identification of modal properties of bridges. Journal of Structural Engineering, 1990, 116(7), pp. 2008-2021.

[10] Pandey AK, Biswas M, Samman MM. Damage detection from changes in curvature mode shapes. Journal of sound and vibration, 1991, 145(2), pp. 321-332.

[11] Foti, D. Dynamic identification techniques to numerically detect the structural damage. The Open Construction and Building Technology Journal, 2013, 7(1), pp. 43-50.

[12] Wahab M A, De Roeck G. Damage detection in bridges using modal curvatures: application to a real damage scenario. Journal of Sound and Vibration, 1999, 226(2), pp. 217-235.

[13] Pandey A K, Biswas M. Experimental verification of flexibility difference method for locating damage in structures. Journal of Sound and Vibration, 1995, 184(2), pp. 311-328.

[14] Zhang Z, Aktan A E. The damage indices for the constructed facilities. In Proceedings-spie the International Society for Optical Engineering, 1995, pp. 1520-1520.

[15] Cunha Á, Caetano E. From input-output to output-only modal identification of civil engineering structures. In 1st International Operational Modal Analysis Conference (IOMAC), 2005.

[16] Greiner B. Operational modal analysis and its application for SOFIA telescope assembly vibration measurements, 2009, PhD Thesis, Institute of Space Systems, Stuttgart.

[17] Ghalishooyan M, Shooshtari A. Operational Modal Analysis Techniques and their Theoretical and Practical Aspects: A Comprehensive Review and Introduction. In 6th International Operational Modal Analysis Conference IOMAC, 2015.

[18] Basseville M, Benveniste A, Goursat M, Hermans L, Mevel L, Van der Auweraer H. Output-only subspace-based structural identification: from theory to industrial testing practice. Journal of Dynamic Systems, Measurement, and Control, 2001, 123(4), pp. 668-676.

[19] Peeters B, De Roeck G. Reference based stochastic subspace identification in civil engineering. Inverse Problems in Engineering, 2000, 8(1), pp. 47-74.

[20] Xie Y, Liu P, Cai G P. Modal parameter identification of flexible spacecraft using the covariance-driven stochastic subspace identification (SSI-COV) method. Acta Mechanica Sinica, 2016, 32(4), pp. 710-719.

[21] Peeters B, De Roeck G, Pollet T, Schueremans L. Stochastic subspace techniques applied to parameter identification of civil engineering structures. Proceedings of New Advances in Modal Synthesis of Large Structures: Nonlinear, Damped and Nondeterministic Cases, Lyon, France, 1995, pp. 145-156.

[22] Kuts VA, Nikolaev SM, Voronov SA. The procedure for subspace identification optimal parameters selection in application to the turbine blade modal analysis. Procedia Engineering, 2017, 176, pp. 56-65.

[23] Brincker R, Zhang L, Andersen P. Modal identification from ambient responses using frequency domain decomposition. In Proc. of the 18th International Modal Analysis Conference (IMAC), San Antonio, Texas, 2000.

[24] Wang T, Celik O, Catbas FN, Zhang LM. A frequency and spatial domain decomposition method for operational strain modal analysis and its application. Engineering Structures, 2016, 114, pp. 104-112.

[25] Gade S, Møller NB, Herlufsen H, Konstantin-Hansen H. Frequency domain techniques for operational modal analysis. In 1st IOMAC Conference, 2005.

[26] Talbot M, Laflamme JF, Savard M. Approches expérimentales et numériques pour l'analyse dynamique d'un pont routier. Revue Européenne de Génie Civil, 2005, 9(1-2), pp. 187-214.

[27] Jankowiak T, Lodygowski T. Identification of parameters of concrete damage plasticity constitutive model. Foundations of civil and environmental engineering, 2005, 6(1), pp. 53-69.